

Proceedings of the International CFIC 96 Conference

Fractals and Chaos in Chemical Engineering

Rome, Italy

2 – 5 September 1996

editors

M Giona

Università di Cagliari

G Biardi

Polltecnico di Milano



World Scientific

Singapore • New Jersey • London • Hong Kong

Published by

World Scientific Publishing Co. Pte. Ltd.

P O Box 128, Farrer Road, Singapore 912805

USA office: Suite 1B, 1060 Main Street, River Edge, NJ 07661

UK office: 57 Shelton Street, Covent Garden, London WC2H 9HE

British Library Cataloguing-in-Publication Data

A catalogue record for this book is available from the British Library.

FRACTALS AND CHAOS IN CHEMICAL ENGINEERING

Copyright © 1997 by World Scientific Publishing Co. Pte. Ltd.

All rights reserved. This book, or parts thereof, may not be reproduced in any form or by any means, electronic or mechanical, including photocopying, recording or any information storage and retrieval system now known or to be invented, without written permission from the Publisher.

For photocopying of material in this volume, please pay a copying fee through the Copyright Clearance Center, Inc., 222 Rosewood Drive, Danvers, MA 01923, USA. In this case permission to photocopy is not required from the publisher.

ISBN 981-02-3165-2

Printed in Singapore.

PREFACE

The CFIC 96 Conference (Rome, September 2-5, 1996) is the second meeting on fractals and chaos and their applications in chemical engineering organized by the Italian Research Center on Disordered Systems and Fractals in Chemical Engineering, jointly founded in 1993 by the Departments of Chemical Engineering of the Universities of Cagliari, Genoa and Rome and the Polytechnic Institute of Milan.

The CFIC 96 Conference was attended by over 100 researchers and students from all countries and all research fields. The original goal of organizing a working conference to facilitate the interdisciplinary exchange of ideas and to address the most relevant applications of dynamical and disordered system theory in reaction engineering, chemical physics and catalysis can, with no undue rhetoric, be described as successfully achieved. The very positive and in some cases enthusiastic response of many participants was the best reward for the great organizational effort involved. Special thanks for making it possible to organize this conference go to the entire group of the University of Rome, and to A.R. Giona, A. Adrover and O. Patierno in particular.

This book contains the articles presented at the conference and accepted for publication after a peer-reviewing procedure. These articles are fully representative of the intense and scientifically rich program of the Conference. The articles are divided into different sections representing the main fields of application of fractal and chaos theory in chemical engineering science.

Special thanks go to the members of the Scientific Committee (P.M. Adler, D. Avnir, F. Brouers, M.-O. Coppens, J. Drahos, R. Krishna, R. Lapasin, F. Muzzio, W. Rudzinski, W.A. Schwalm, T. Vicsek) and to the referees for their cooperation in the preparation of this book. The financial support of the CNR (Consiglio Nazionale delle Ricerche, Comitato per la Chimica) is gratefully acknowledged.

Massimiliano Giona and Giuseppe Biardi
Chairmen of CFIC 96 Conference

CONTENTS

Preface	v
---------------	---

Transport, Reaction, Adsorption in Disordered Systems

The influence of spatial correlations on reaction/diffusion and convective transport phenomena	3
<i>A. Adrover and A. Galassini</i>	
A comparison of reaction rates in mass fractal and nonfractal catalysts	15
<i>M.-O. Coppens and G. F. Froment</i>	
Oxidation processes and fractal properties of activated carbons	27
<i>F. Ehrburger-Dolle, T. Rieker, M.T. Gonzalez, M. Molina-Sabio, F. Rodriguez-Reinoso, P. Pfeifer and P. W. Schmidt</i>	
Transport properties of diluted simple-cubic networks of capillaries	39
<i>S. P. Friedman and N. A. Seaton</i>	
Exact solution of transport schemes in the presence of a multifractal distribution of transport/reaction coefficients	56
<i>M. Giona and A. Adrover</i>	
Perspectives and applications of Green function renormalization with respect to transport phenomena	68
<i>M. Giona, W. A. Schwalm, M. K. Schwalm and A. Adrover</i>	
Adsorption kinetics on fractal surfaces: an approximate mean-field model	80
<i>M. Giustiniani and M. Giona</i>	
Localization of electrons in loopless fractals	91
<i>J. W. Kantelhardt, H. E. Roman and A. Bunde</i>	
Randomness and apparent fractality	103
<i>D. A. Lidar (Hamburger), O. Malcai, O. Biham and D. Avnir</i>	
Electronic structure of the <i>dauidene</i> : the physics of a fractal carbon aggregate ..	115
<i>A. Lorenzoni, H.E. Roman, G. Benedek and R. A. Broglia</i>	
Percolative fragmentation during the gasification of carbons	127
<i>F. Miccio, R. Chirone and P. Salatino</i>	
Fractal characterization of the devil's comb by random walk simulations	139
<i>P. Mougin, M. Pons and J. Villermaux</i>	
Screening transition in diffusion to and across fractal surfaces	151
<i>P. Pfeifer and P. J. Hagerty</i>	
Wavelet analysis for Anderson wavefunctions in one and two dimensions	165
<i>H. E. Roman and J. W. Kantelhardt</i>	
Chaos and correlations in mixed-gas adsorption on the real solid surfaces	175
<i>W. Rudziński and K. Nieszporek</i>	
Diffusion of material and energy on Vicsek and related lattices	187
<i>M. K. Schwalm, D. K. Ludlow and H. Ni</i>	

Group theoretic reduction of discrete diffusion equations on regular fractal structures	199
<i>W. A. Schwalm, M. K. Schwalm and M. Giona</i>	
Immiscible displacement processes in porous media	211
<i>A. M. Viales, G. Zgrablich, E. N. Miranda and M. Rosen</i>	

Aggregates and Growth Models

Aggregate structure effects from a bimodal primary particle size distribution ..	225
<i>G. C. Bushell, R. Amal and J. A. Raper</i>	
Hydrodynamic drag on suspensions of fractal aggregates	234
<i>D. Coelho, J.-F. Thovert, R. Thoy and P. M. Adler</i>	
Dynamic scaling of growing surfaces and interfaces	246
<i>F. Family</i>	
Fractal analysis of gap in two-dimensional pattern of silver halide film	286
<i>Y. Hasegawa and S. Miyazima</i>	
Domain wall roughening in disordered media: from local spin dynamics to a continuum description of the interface	293
<i>M. Jost and K. D. Usadel</i>	
Thixotropy in fractal and dense aggregate suspensions	305
<i>R. Lapasin, M. Grassi and S. Prigl</i>	
Fractal properties of Eden growth surface with acceleration points	317
<i>T. Nagamine and S. Miyazima</i>	
Diffusion-convection effects in surface decay processes	326
<i>A. P. Reverberi and M. S. Fumagalli</i>	
Cluster structure for off-lattice percolation at criticality	333
<i>H. E. Roman and M. Meyer</i>	
Multifractal analysis of dipmeter well logs for characterization of geological structures	345
<i>A. Saucier, O. K. Huseby and J. Muller</i>	

Turbulence, Mixing and Spatiotemporal Patterns

Scaling properties of tracer trajectories in a three-dimensional saturated porous medium by means of stereoscopic PTV technique	359
<i>A. Cenedese, M. Moroni and P. Viotti</i>	
Scaling gyroscopes cascade: universal multifractal features of 2-d and 3-d turbulence	371
<i>Y. Chigirinskaya, D. Schertzer and S. Lovejoy</i>	
Characterization of strange attractors in the self-ignition of coal stockpiles	385
<i>G. Continillo, G. Galiero, P. L. Maffettone and S. Crescitelli</i>	
Chaotic dynamics of bubble formation in a pool of liquid	397
<i>J. Drahoš, M. C. Ruzicka, V. Pěnkavová and C. Serio</i>	

Bifurcation analysis of the rigid rod model for nematic polymers in shear flows	409
<i>V. Faraoni, P. L. Maffettone and S. Crescitelli</i>	
Predictability of multifractal processes: the case of turbulence	421
<i>D. Marsan, D. Schertzer and S. Lovejoy</i>	
Using concepts from dynamical systems theory to understand and enhance mixing in industrial processes	434
<i>F. J. Muzzio, D. M. Hobbs, D. J. Lamberto, C. Wightman and D. Brone</i>	
Reactive chaotic flows	451
<i>F. J. Muzzio and M. Liu</i>	
Multifractal properties of temperature fluctuations in turbulence	464
<i>F. Schmitt, D. Schertzer, S. Lovejoy and Y. Brunel</i>	
Fluctuation-dominated kinetics under regular and turbulent flows	476
<i>I. M. Sokolov, R. Reigada, F. Sagués, J. M. Sancho and A. Blumen</i>	

Reactor Dynamics and Chaos

Periodicity and aperiodicity in externally forced industrial FCC units	489
<i>A. E. Abasaed and S.S.E.H. Elnashaie</i>	
Chaotic behavior of a non-isothermal fluidized bed catalytic reactor under conventional PID control	500
<i>A. Ajbar, K. Alhumaizi and S.S.E.H. Elnashaie</i>	
Neural networks for prediction and control of chaotic fluidized bed hydrodynamics: a first step	512
<i>R. Bakker, R. J. De Korte, J.C. Schouten and C.M. Van den Bleek</i>	
Multidimensional mapping representation by multiple 1-dimensional decomposition for complex systems modelling	518
<i>R. Carotenuto, L. Franchina and M. Coli</i>	
Bifurcation and its implications on industrial UNIPOL process for the production of polyethylene in fluidized bed catalytic reactors	530
<i>S.S.E.H. Elnashaie, N. M. Ghasem and R. Hughes</i>	
Discrete adaptive control of oscillatory and chaotic systems	542
<i>A. L. Fradkov, P. Yu. Guzenko, S. A. Kukushkin and A. V. Osipov</i>	
Gradient control of one and two dimensional discrete time systems	554
<i>P. Yu. Guzenko</i>	
Chaotic behavior of a pseudo-homogeneous floc model of a bioreactor	566
<i>G. Ibrahim and A. Ajbar</i>	
The dynamics of equation solving	578
<i>A. Lucia and D. Liu</i>	
Chaos in systems with chemical reaction - mass transport interactions	590
<i>M. Marek, P. Hasal, I. Schreiber and A. F. Münster</i>	
Adaptive synchronization of coupled chaotic systems	628
<i>A. Yu. Markov and A. L. Fradkov</i>	

A Monte Carlo method for the stability analysis of an ideal PI controlled CSTR performing a ν -order exothermic reaction	640
<i>M. Ratto and O. Paladino</i>	
Nonlinear dynamics of a fixed bed reactor with recycle	652
<i>B. O. Recke and S. B. Jorgensen</i>	
The OGY method in the case of a PI controlled CSTR. Part I: comparison of different ways of building up the method	664
<i>C. Tablino Possio, L. Pellegrini, S. Albertoni</i>	
The OGY method in the case of PI controlled CSTR. Part II: effects of noise ..	676
<i>L. Pellegrini, C. Tablino Possio and G. Biardi</i>	
Bifurcation behaviour of industrial fixed bed catalytic reactors for the production of phthalic anhydride	688
<i>K. M. Wagialla and S.S.E.H. Elnashaie</i>	
Subject index	701
Author index	706
List of contributors	709

Transport, Reaction, Adsorption in Disordered Systems

The influence of spatial correlations on reaction/diffusion and convective transport phenomena

Alessandra Adrover and Alessandro Galassini

*Dipartimento di Ingegneria Chimica
Università di Roma "La Sapienza"
Via Eudossiana 18, 00184 Rome, Italy*

The article analyzes the influence of the spatial correlation of the pore structure on reaction-diffusion and convective transport phenomena. Two aspects are developed in greater detail: prediction of the permeability of correlated porous structures and the influence of correlations in fluid-solid noncatalytic reactions. A general purpose simulator for fluid-solid reaction in complex geometries is also proposed.

1 Introduction

Random percolation networks are an important tool for modeling transport processes in disordered systems such as porous media, polymers and gels. In the study of percolation models, spatial disorder is usually assumed to be uncorrelated, i.e. the probability of any site being occupied is independent of the occupancy of other sites. However, natural systems exhibit some degree of spatial correlation, and correlated percolation models^{1,2} prove to be useful in application to porous media and transport because they mimic the structure of real materials³ better than the customary uncorrelated percolation schemes.

The generation of correlated percolation lattices can be regarded as an application of the *reconstruction of porous media*. This topic has been extensively studied by Joshi⁴, Quiblier⁵, Adler et al.³. An analytic solution of the inverse reconstruction problem has recently been proposed by Giona and Adrover⁶ for isotropic and homogeneous porous media and further extended to the generation of non homogeneous porous matrices with prescribed pore-pore correlation function and position-dependent porosity⁷.

The purpose of this article is to analyze the influence of the spatial correlations of the pore network on reaction/diffusion and convective transport phenomena. In particular, we review the main results of the permeability model for correlated porous structures proposed by Adrover and Giona⁸ and analyze the influence of the spatial correlation of solid reactant distribution on fluid-solid noncatalytic reactions, presenting an efficient lattice simulator for diffusion and reaction phenomena in the presence of moving boundary conditions.

2 Generation of correlated percolation lattices

Let us consider a thin section of a porous medium as a two-dimensional image \mathcal{I} , and let \mathcal{P} be the pore space, described by its characteristic function $\chi_{\mathcal{P}}(\mathbf{x})$, such that $\chi_{\mathcal{P}}(\mathbf{x}) = 1$ if $\mathbf{x} \in \mathcal{P}$ and $\chi_{\mathcal{P}}(\mathbf{x}) = 0$ elsewhere.

The porosity ε is given by $\varepsilon = \langle \chi_{\mathcal{P}}(\mathbf{x}) \rangle$, and the normalized pore-pore correlation function by

$$C_{2\chi}(\mathbf{x}) = \frac{\langle (\chi_{\mathcal{P}}(\mathbf{y}) - \varepsilon)(\chi_{\mathcal{P}}(\mathbf{y} + \mathbf{x}) - \varepsilon) \rangle}{\varepsilon - \varepsilon^2}. \quad (1)$$

On the assumption of isotropy, $C_{2\chi}(\mathbf{x})$ is solely a function of $x = |\mathbf{x}|$ and a generic cross section of the material is representative of the entire three-dimensional structure. The goal of the reconstruction of porous media is to generate stochastic lattice models with the same porosity and the same pore-pore correlation function as the original image. The methods developed to solve the reconstruction problem⁶ can be applied to generate percolation models with correlations by assuming a given functional expression for the pore-pore correlation function and by letting the porosity vary.

Let us define the set of basis processes $\{\mathcal{Y}(\mathbf{x}, \lambda)\}$ by convoluting a system of Gaussian uncorrelated processes $\xi_{\lambda}(\mathbf{x})$ (with zero mean and unit variance) with a Gaussian kernel,

$$\mathcal{Y}(\mathbf{x}, \lambda) = \int_{E^d} a(\mathbf{u}, \lambda) \xi_{\lambda}(\mathbf{u} + \mathbf{x}) d\mathbf{u} = \left(\frac{4\lambda}{\pi} \right)^{d/4} \int_{E^d} e^{-2\lambda \mathbf{u}^2} \xi_{\lambda}(\mathbf{u} + \mathbf{x}) d\mathbf{u}, \quad (2)$$

where E^d is the Euclidean d -dimensional space, $E^d = \{\mathbf{x} \mid -\infty < x_i < \infty, (i = 1, \dots, d)\}$. Each basis process $\mathcal{Y}(\mathbf{x}, \lambda)$ is still Gaussian with zero mean and unit variance but exhibits a Gaussian decay of the correlation function^a $C_{2\mathcal{Y}}(\mathbf{x}, \lambda) = e^{-\lambda x^2}$.

We can expand a generic Gaussian process $\mathcal{Y}(\mathbf{x})$ as the linear superposition^{6,8} of a continuous and a discrete spectrum of basis process $\{\mathcal{Y}(\mathbf{x}, \lambda)\}$

$$\mathcal{Y}(\mathbf{x}) = \int_0^{\infty} \hat{p}(\lambda) \mathcal{Y}(\mathbf{x}, \lambda) d\lambda + \sum_{i=1}^{N_{loc}} \sqrt{\alpha_i} \mathcal{Y}(\mathbf{x}, \lambda_i), \quad (3)$$

which admits the correlation function

$$C_{2\mathcal{Y}}(x) = \int_0^{\infty} \hat{\pi}(\lambda) e^{-\lambda x^2} d\lambda + \sum_{i=1}^{N_{loc}} \alpha_i e^{-\lambda_i x^2}, \quad (4)$$

^aThe basis processes $\{\mathcal{Y}(\mathbf{x}, \lambda)\}$ for different λ are uncorrelated with one another, i.e. $\langle \mathcal{Y}(\mathbf{x}, \lambda_1) \mathcal{Y}(\mathbf{x}', \lambda_2) \rangle = 0$ for $\lambda_1 \neq \lambda_2$.

where N_{loc} is the number of discrete (localized) Gaussian contributions and $\hat{\pi}(\lambda) = \hat{p}^2(\lambda)$.

The entire spectrum $\pi(\lambda)$ of λ encompassing both the continuous and the discrete part is given by $\pi(\lambda) = \hat{\pi}(\lambda) + \sum_{i=1}^{N_{loc}} \alpha_i \delta(\lambda - \lambda_i)$.

The transformation from the \mathcal{Y} -process to the binary (pore/pore matrix, 0/1) porous structure with a given value of the porosity ε is given by a nonlinear filter^{3,6} \mathcal{G} depending on the Gaussian distribution function $F_{\mathcal{Y}}$ of \mathcal{Y} and on the assigned porosity ε .

For each point \mathbf{x} , the characteristic function of the generated (0/1) porous structure $\chi_{\mathcal{P}}(\mathbf{x})$ is given by

$$\chi_{\mathcal{P}}(\mathbf{x}) = \mathcal{G}(\mathcal{Y}(\mathbf{x}), \varepsilon) = \begin{cases} 1 & F_{\mathcal{Y}}(\mathcal{Y}(\mathbf{x})) < \varepsilon \\ 0 & F_{\mathcal{Y}}(\mathcal{Y}(\mathbf{x})) > \varepsilon \end{cases} \quad (5)$$

Eq. (5) ensures statistically that the generated porous medium admits the porosity ε , while the correlation function $C_{2\chi}(x)$ is related to the corresponding correlation function $C_{2\mathcal{Y}}(x)$ through the relation^{3,6}

$$C_{2\chi}(x) = \int_{-\infty}^{\infty} dy_1 \int_{-\infty}^{\infty} dy_2 \left[\frac{(\mathcal{G}(y_1, \varepsilon) - \varepsilon)(\mathcal{G}(y_2, \varepsilon) - \varepsilon)}{\varepsilon - \varepsilon^2} \right] p(y_1, y_2, C_{2\mathcal{Y}}(x)) , \quad (6)$$

where $p(y_1, y_2, C_{2\mathcal{Y}}(x))$ is a bivariate Gaussian p.d.f. with correlation coefficient $C_{2\mathcal{Y}}(x)$.

In order to generate a lattice structure possessing a specified porosity and a given functional expression of $C_{2\chi}(x)$, for every $C_{2\chi}(x)$, the corresponding value of $C_{2\mathcal{Y}}(x)$ is evaluated through eq. (6). From the knowledge of $C_{2\mathcal{Y}}(x)$, the weight function $\pi(\lambda)$ can be evaluated numerically or analytically (where possible) from eq. (4).

It should be observed that, on the condition that $C_{2\mathcal{Y}}(x) \geq 0$, and putting $z = x^2$, $\tilde{C}_{2\mathcal{Y}}(z) = C_{2\mathcal{Y}}(x)$,

$$\tilde{C}_{2\mathcal{Y}}(z) = \int_0^{\infty} \pi(\lambda) e^{-\lambda z} d\lambda , \quad (7)$$

it follows that $\pi(\lambda)$ is the inverse Laplace transform of the analytic continuation on the complex plane $\tilde{C}_{2\mathcal{Y}}^{(p)}(z)$ of the correlation function of the $\mathcal{Y}(\mathbf{x})$ process^b $\tilde{C}_{2\mathcal{Y}}(z)$. In all those cases in which closed-form solutions for the inverse Laplace transform of $\tilde{C}_{2\mathcal{Y}}^{(p)}(z)$ cannot be obtained, the weight function $\pi(\lambda)$ should be obtained numerically.

^bThe analytic continuation $\tilde{C}_{2\mathcal{Y}}^{(p)}(z)$ of $\tilde{C}_{2\mathcal{Y}}(z)$ valid for all complex z (whose restriction to real z coincides with $\tilde{C}_{2\mathcal{Y}}(z)$) can be achieved by considering rational approximations (Padé approximants) or by means of other methods such as orthogonal polynomial expansion⁶.

3 Permeability of correlated percolation lattices

In section 2 we have shown that a generic correlated porous structure can be generated by means of the linear superposition of basis processes $\{\mathcal{Y}(\mathbf{x}, \lambda)\}$ possessing a Gaussian decay in the correlation function $C_{2\mathcal{Y}}(x)$. Henceforth we shall refer to these structures as Gaussian correlated percolation lattices.

In ref. [8] an analogous superposition principle is applied to predict transport properties, and specifically permeability. Starting from the study of the permeability of random lattices generated by an elementary basis process $\mathcal{Y}(\mathbf{x}, \lambda)$, an equation can be derived for the permeability of random structures generated by the superposition of the basis processes $\{\mathcal{Y}(\mathbf{x}, \lambda)\}$.

For 2- d lattice structures, the Carman-Kozeny equation⁹ for permeability attains the form

$$\frac{K}{a^2} = \frac{N^4}{k_{koz}} \frac{\varepsilon^3}{(w_p/a)^2}, \quad (8)$$

where N is the lattice size expressed in lattice units, a the unit lattice site length, and w_p/a the dimensionless wetted perimeter.

For Gaussian correlated percolation lattices, the dimensionless wetted perimeter w_p/a behaves as $w_p/a \sim N^2 \sqrt{1 - \varepsilon} (a\sqrt{\lambda_1})$, and the Carman-Kozeny equation attains the form

$$\frac{K}{a^2} = \frac{1}{k_\lambda} \frac{\varepsilon^3}{(1 - \varepsilon)(\lambda_1 a^2)}, \quad (9)$$

in which k_λ is a modified Kozeny constant.

Figure 1 shows the comparison of the theoretical curve eq. (9) and the Lattice Boltzmann Equation (LBE)¹⁰ simulation results^c for the permeability K/a^2 as a function of $\varepsilon^3/((1 - \varepsilon)\lambda_1 a^2)$ for many different exponentially correlated lattice structures with $0.70 \leq \varepsilon \leq 0.90$ and $0.01 \leq \lambda_1 a^2 \leq 0.20$. This figure clearly shows that the Carman-Kozeny relation expressed as a function of λ_1 , eq. (9), is well verified by exponentially correlated percolation lattices far from criticality with a unique value of the modified Kozeny constant $k_\lambda = 13.5 \pm 0.3$.

In order to develop a predictive model for the permeability of random correlated lattice structures, eq. (9) should be generalized for arbitrary structures possessing a discrete and/or continuous spectrum $\pi(\lambda)$, eq. (4).

^cLattice Gas Automata (LGA) and the Lattice Boltzmann Equation (LBE) have been developed as an alternative method to direct simulation and to spectral techniques for solving the partial differential equations of fluid mechanics and transport. The ease with which arbitrary complex boundary conditions are handled by the LBE approach prompts its use to tackle a great variety of problems related to the physics and fluid dynamics of disordered and fractal media.

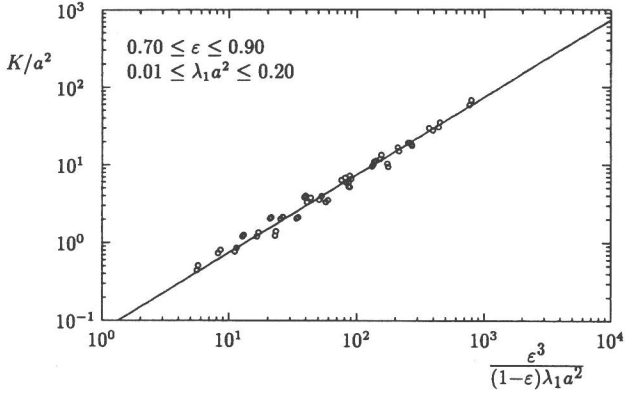


Figure 1: LBE simulation results for the permeability K/a^2 of two different sets of 200×200 exponentially correlated percolation lattices ($0.01 \leq \lambda_1 a^2 \leq 0.20$) far from criticality ($0.70 \leq \epsilon \leq 0.90$). The continuous line corresponds to eq. (9) with a least square fitted value of the modified Kozeny constant $k_\lambda = 13.5$.

By considering that the correlation function of a lattice structure generated as a linear superposition of the basis processes $\{\mathcal{V}(\mathbf{x}, \lambda)\}$ is a linear superposition of the correlation functions $C_{2\mathbf{y}}(\mathbf{x}, \lambda)$, it is natural to extend eq. (9) in the form

$$\frac{K}{a^2} = \frac{1}{k_\lambda} \frac{\epsilon^3}{(1 - \epsilon) \langle \lambda \rangle a^2}, \quad (10)$$

where $\langle \lambda \rangle$ is the average of λ , with respect to the spectrum $\pi(\lambda)$

$$\langle \lambda \rangle = \int_0^\infty \lambda \pi(\lambda) d\lambda = \int_0^\infty \lambda \tilde{\pi}(\lambda) d\lambda + \sum_{i=1}^{N_{loc}} \alpha_i \lambda_i. \quad (11)$$

and k_λ is the same modified Kozeny constant estimated in the previous section for exponentially correlated structures.

Eqs. (10) and (11) enable us to predict the permeability of generic 2- d porous structures from their structural data. From the knowledge of the experimental $C_{2\mathbf{x}}(\mathbf{x})$ and of ϵ , we calculate $\tilde{C}_{2\mathbf{y}}(z)$ by using eq.(6) and then estimate $\pi(\lambda)$ numerically as the inverse Laplace transform of the analytic continuation on the complex plane of $\tilde{C}_{2\mathbf{y}}(z)$.

Once ϵ , $\pi(\lambda)$ and consequently $\langle \lambda \rangle$ are known, we calculate K/a^2 from eq. (10) with the same value of the modified Kozeny constant k_λ estimated from the analysis of exponentially correlated percolation lattices.

To validate the model, we predict the permeability of deterministic and stochastic fractal structures at different iterations in the construction process,

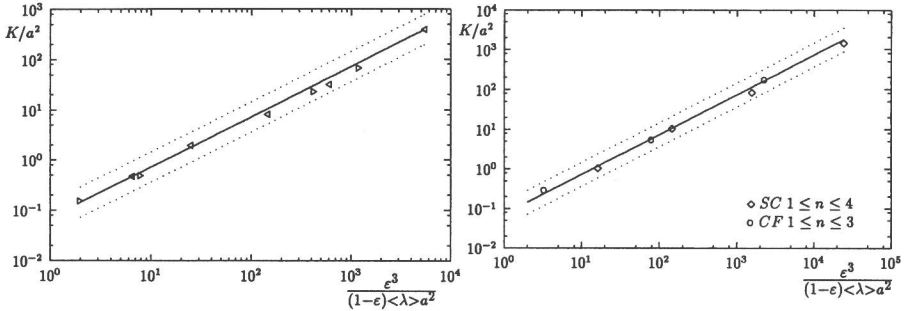


Figure 2: LBE simulation results for the permeability K/a^2 vs $\epsilon^3/((1-\epsilon)\langle\lambda\rangle a^2)$ for probabilistic and stochastic fractal structures at different iterative construction stages: a) two different realizations of a fractal percolation lattice ($b=2$, $p=0.90$, $N=256$) for $3 \leq n \leq 7$; b) Sierpinsky Carpet ($1 \leq n \leq 4$) and Chess Fractal ($1 \leq n \leq 3$). The continuous line is the model, eq.(11). Dotted lines correspond to an error of factor two, i.e. an error bounded between $K_{model}/2 \leq K \leq 2K_{model}$.

and compare the model predictions with LBE simulation results. The stochastic structures considered are fractal percolation lattices¹¹. The deterministic fractal structures are the Sierpinski Carpet (SC) and the Chess Fractal (CF)⁸, specifically designed since, unlike the Sierpinski carpet, it does not exhibit straight channels. A fractal percolation lattice is a random fractal generated by means of an iterative procedure. The square lattice $\mathcal{E}_0 = N \times N$ is divided into b^2 squares of side N/b (in lattice units). A subset of these squares is selected to form \mathcal{E}_1 in such a way that each square has the independent probability p of being chosen as a square of \mathcal{E}_2 . The iterative procedure continues so that \mathcal{E}_n is a random collection of squares of side $\delta_n = N/b^n$ (in lattice units).

This iterative procedure, which depends on the parameters p and b , defines a random fractal $\mathcal{F}_{p,b} = \cap_{n=0}^{\infty} \mathcal{E}_n$ with fractal dimension $D = \log(b^2 p)/\log(b)$.

The deterministic fractals analyzed are generated by means of a similar but deterministic iterative procedure. The square lattice $\mathcal{E}_0 = N \times N$ is divided into b^2 squares of side N/b . A set of $(b^2 - l^2)$ of these squares is selected to form \mathcal{E}_1 . The iterative procedure continues so that \mathcal{E}_n is a collection of squares of side $\delta_n = N/b^n$.

For all the lattice structures generated by means of an iterative procedure, the evaluation of $\langle\lambda\rangle$ should take into account the fact that at each iteration there exists a well-defined minimum dissipation lengthscale controlling the viscous effects at the solid boundary. This minimum dissipation length corre-

sponds to the lattice side $\delta_n = N/b^n$ of the smallest box at the iteration n . The existence of such a lengthscale implies that there exists a limiting value λ_c of λ , $a^2\lambda_c = 4/\delta_n^2$, such that all the values of $\lambda > \lambda_c$ are not related to viscous transport phenomena.

Consequently, eq. (11) should be reformulated as

$$\langle \lambda \rangle = \frac{\int_0^{\lambda_c} \lambda \hat{\pi}(\lambda) d\lambda + \sum_{i=1}^{\bar{N}_{loc}} \alpha_i \lambda_i}{\int_0^{\lambda_c} \hat{\pi}(\lambda) d\lambda + \sum_{i=1}^{\bar{N}_{loc}} \alpha_i}, \quad (12)$$

\bar{N}_{loc} being the number of localized Gaussian contributions with $\lambda_i \leq \lambda_c$.

Figures 2 a)-b) show the excellent agreement between the theoretical curve eq. (10) and the LBE simulation results of permeability for (a) two realizations of fractal percolation lattices ($b = 2$, $p = 0.90$, $N = 256$) and (b) the two deterministic fractals SC ($b = 3$, $l = 1$, $D = \log(8)/\log(3)$, $N = 243$) and CF ($b = 4$, $l = 2$, $D = \log(12)/\log(4)$, $N = 256$), at different iteration stages. The value of k_λ is the same obtained from the analysis of exponentially correlated percolation lattices, $k_\lambda = 13.5$.

Although the model has been derived from the Carman-Kozeny equation applied to exponentially correlated percolation lattices, its range of application and quantitative prediction capabilities are greater than the Carman-Kozeny model. Without any fitting parameters, the model predicts with great accuracy the permeability of highly diluted exponentially correlated percolation lattices ($0.93 \leq \varepsilon \leq 0.995$) and also the permeability of a 2- d square array of cylinders throughout the entire range of the solid fraction c , including the range of c in which the Carman equation fails, i.e. for very concentrated and very diluted arrays.

4 Fluid-solid noncatalytic reactions

The literature on gas-solid noncatalytic reactions¹² usually considers two distinct phenomenologies: (a) the particle is initially non-porous and the solid reactant is distributed in an inert matrix; fluid diffuses through the product layer and reaction occurs at a moving boundary; (b) the particle is initially porous and reaction occurs in a distributed way throughout the entire pore-space. For both phenomenologies, many authors have analyzed the influence of the spatial distribution of solid reactant^{13,14,15} on the conversion vs time curves, regardless of the spatial correlation properties. We study the influence of the spatial correlation of the solid reactant on fluid-solid non-catalytic reactions, focusing on initially non-porous particles with an assigned solid reactant distribution function.